University of Groningen

Influence of polydispersity on the phase behavior of statistical multiblock copolymers with Schultz-Zimm block molecular weight distributions

Angerman, H.J.; Brinke, G. ten; Slot, J.J.M.

[Link to publication in University of Groningen/UMCG research database](#)

Influence of polydispersity on the phase behavior of statistical multiblock copolymers with Schultz-Zimm block molecular weight distributions

H.J. Angerman[1,a], G. ten Brinke[1], and J.J.M. Slot[2]

[1] Department of Polymer Chemistry and Materials Science Centre, University of Groningen, Nijenborgh 4, 9747 AG, Groningen, The Netherlands

[2] Department for Physical, Analytical and Computational Chemistry, DSM Research, P.O. Box 18, 6160 MD, Geleen, The Netherlands

Abstract. In this paper we investigate in a systematic way the influence of polydispersity in the block lengths on the phase behavior of AB-multiblock copolymer melts. As model system we take a polydisperse multiblock copolymer for which both the A-blocks and the B-blocks satisfy a Schultz-Zimm distribution. In the limit of low polydispersity the expressions for the vertex functions are clarified by using simple physical arguments. For various values of the polydispersity the phase diagram is presented, which shows that the region of stability of the bcc phase increases considerably with increasing polydispersity. The strong dependence of the periodicity of the microstructure on the polydispersity and on the interaction strength is presented.

PACS. 61.41.+e Polymers, elastomers, and plastics

1 Introduction

Heterogeneous polymer melts may undergo a phase transition driven by an unfavourable interaction between the different monomer types. In homopolymer blends this phase transition leads to a state where the system is separated into coexisting phases (macrophase separation). In copolymer melts, on the other hand, monomers of different type are chemically connected within one chain. These monomers cannot be separated over macroscopic distances, and in order to reduce the number of unfavourable interactions the system may undergo a transition to a *micro*phase separated state, which is a locally inhomogeneous state in which the concentration profiles of the various monomer types are periodic functions of space. In order to study microphase separation theoretically, the monodisperse diblock copolymer melt has served as a model system [1–4]. However, many polymerization techniques automatically lead to a certain degree of polydispersity in the block lengths. Also, many industrially important block copolymers, such as thermoplastic elastomers, are highly polydisperse multiblock copolymers (polydisperse not only in overall molecule length, but also in block length). In [5], the influence of polydispersity on the spinodal and its influence on the position q_0 of the minimum of the second order vertex was investigated for

various architectures such as linear, combs and stars. The aim of the present paper is to investigate systematically the influence of polydispersity on the position of the phase transition lines, the stability of the various microstructures, and the periodicity (note that in general the parameter q_* determining the periodicity might differ from q_0; see for instance [6]). Also, we intend to provide some physical insight in the complicated expressions for the vertex functions of polydisperse multiblock copolymers. As a model system we take a two-component polydisperse AB-multiblock copolymer for which both the lengths of the A-blocks, and the lengths of the B-blocks satisfy a Schultz-Zimm distribution (to be defined in Sect. 2). This distribution contains a free parameter that controls the degree of polydispersity. The system will be studied in the weak segregation regime, where the separation between the A- and B-monomers is not complete. In the phase diagram this corresponds to the region in the vicinity of the critical point. The calculations will be done in the mean-field approximation, which is reasonable provided that the block lengths are not too short [3]. The procedure consists of deriving an expression for the Landau free energy, and subsequently minimizing it with respect to the amplitude, the period, and the type of the microstructure [1]. For monodisperse melts the expression for the Landau free energy was derived in [1]. In order to obtain the corresponding expression for polydisperse melts, it was shown in [7] that the ideal intra-chain correlation functions have

[a] e-mail: `angerman@chem.rug.nl`

to be averaged over the polydispersity, after which the vertex functions can be calculated along the same lines as in the monodisperse case. However, compared to the monodisperse case, the fourth order vertex has an additional contribution, the so-called non-local term, which was derived for the first time in [6] for the case of random copolymers, and later on in its most general form in [8–11]. In [12] the resulting expression for the Landau free energy has been worked out in detail for a rather broad class of linear polydisperse multiblock copolymers. This class encompasses copolymer melts containing an arbitrary number of monomer types. There are only 3 restrictions: the number of blocks per molecule is large; the block lengths are independent of each other; and the order of the different block types is governed by a first order Markov process. The multiblock copolymer studied in this paper belongs to this class, and so we can use the general formulas derived in [12]. The expression for the free energy obtained in this way is, however, rather complicated, and in order to increase physical insight, we will study it in the limit of low polydispersity. In the last section of this paper we present several phase diagrams, revealing the influence of the polydispersity.

2 Model

Consider an incompressible polydisperse multiblock copolymer melt containing two segment types A and B. The excluded volume v per segment, and the statistical segment length a are assumed to be the same for both segment types. By choosing the proper unit of length and by redefining the segments, it is always possible to get

$$v^{1/3} = \frac{a}{\sqrt{6}} = 1. \tag{1}$$

The (average) number $N_{\rm b}$ of blocks per molecule is large, and in the calculations we take the limit $N_{\rm b} \to \infty$. The block lengths, which are independent of each other, satisfy the Schultz- Zimm distribution, which is defined by

$$p_\alpha(n) = \frac{k_\alpha^{k_\alpha} e^{-k_\alpha n/\bar{n}_\alpha} n^{k_\alpha-1}}{\Gamma(k_\alpha) \bar{n}_\alpha^{k_\alpha}} . \tag{2}$$

$p_\alpha(n)$ is the probability that a block of type $\alpha = A/B$ contains n segments, $\bar{n}_\alpha \equiv \int {\rm d}n\, n p_\alpha(n)$ is the average number of segments per block of type α, the parameter $k_\alpha \geq 0$ controls the polydispersity of blocks of type α, and $\Gamma(k)$ is the Gamma function. A useful indication for the polydispersity of a distribution is the value of the parameter $U \geq 0$, which is defined by

$$U = \frac{\overline{(n - \bar{n})^2}}{\bar{n}^2} = \frac{n_{\rm w}}{n_{\rm n}} - 1. \tag{3}$$

$n_{\rm n} = \bar{n}$ is the "number average length", and $n_{\rm w} = \overline{n^2}/\bar{n}$ is the "weight average length". For the Schultz-Zimm distribution one obtains

$$U = \frac{1}{k} . \tag{4}$$

For $k = 1$, the Schultz-Zimm distribution reduces to the exponential Flory distribution. In the literature, a multi-block copolymer for which the block lengths satisfy a Flory distribution is called a *correlated random copolymer*, and its phase behavior has been considered in detail in [13–20]. In the limit $k \to \infty$ (*i.e.*, $U \to 0$) the distribution becomes infinitely narrow. This corresponds to regular, monodisperse multiblock copolymers. In Figure 1 the distribution has been plotted for various values of k.

3 Theory

The coarse grained state of an AB-copolymer melt is described by the concentration profile $\psi(\mathbf{x})$, which is the deviation of the local fraction of A-monomers from the average value:

$$\psi(\mathbf{x}) = \rho_A(\mathbf{x}) - f. \tag{5}$$

In mean-field Landau theory [22] the free energy can be expanded in powers of the Fourier transform $\psi(\mathbf{q})$ of the concentration profile:

$$F_{\rm Landau} = \sum_{n=2}^{4} \frac{1}{n!} \frac{1}{(2\pi)^{3n}}$$
$$\times \int {\rm d}\mathbf{q}_1...{\rm d}\mathbf{q}_n \Gamma_n(\mathbf{q}_1, ..., \mathbf{q}_n)\psi(-\mathbf{q}_1)...\psi(-\mathbf{q}_n). \tag{6}$$

The coefficients in this expansion are called "vertex functions". For these vertex functions, closed expressions can be found in terms of the composition of the system; see for instance [8,10–12]. If the number of molecule types exceeds the number of monomer types, the fourth order vertex has a non-local contribution $\Gamma_4^{\rm nl}$ [6,8–10], whose representation in real space has the form

$$\Gamma_4(\mathbf{x}_1, ..., \mathbf{x}_4) =$$
$$\Gamma_4^{\rm loc}(\mathbf{x}_1, ..., \mathbf{x}_4) + \frac{1}{V}\Gamma_4^{\rm nl}(\mathbf{x}_1 - \mathbf{x}_2, \mathbf{x}_3 - \mathbf{x}_4) + ... \tag{7}$$

The dots represent the remaining two different terms obtained by permuting $\mathbf{x}_1, ..., \mathbf{x}_4$ in $\Gamma_4^{\rm nl}$. The vertex $\Gamma_4^{\rm nl}(\mathbf{x}_1 - \mathbf{x}_2, \mathbf{x}_3 - \mathbf{x}_4)$ is non-local in the sense that its value is independent of the distance between $\frac{1}{2}(\mathbf{x}_1 + \mathbf{x}_2)$ and $\frac{1}{2}(\mathbf{x}_3 + \mathbf{x}_4)$, thus coupling points in space that are arbitrarily far apart. In mean-field theory the phase diagram can be constructed by minimizing the Landau free energy equation (6) with respect to the (periodic) concentration profile $\psi(\mathbf{x})$. In the weak segregation regime (*i.e.*, close to the critical point) the profile is dominated by a single wave vector q_*, and it is justified to make the *first harmonic approximation* by neglecting the contributions from other wave vectors. In this case the expression for $\psi(\mathbf{q})$ becomes [1]

$$\psi(\mathbf{q}) = \frac{AV}{\sqrt{m}} \sum_{\mathbf{Q}}^{*} e^{i\phi_{\mathbf{Q}}} \delta_{\rm K}(\mathbf{q} - \mathbf{Q}) \tag{8}$$
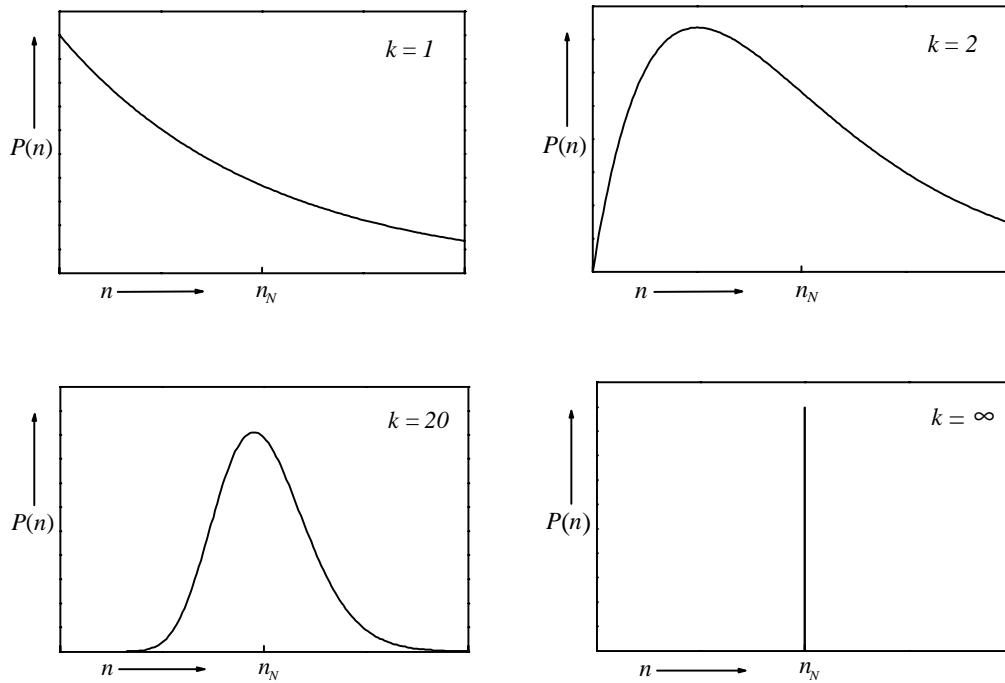
Fig. 1. The Schultz-Zimm distribution for various values of the inverse polydispersity k. Horizontal axis: block length n. Vertical axis: probability density.

where the summation extends over reciprocal lattice vectors, and the star indicates that the summation is restricted to those vectors belonging to the first harmonic sphere; m is half the number of such vectors. A is the amplitude, and $\phi_{\mathbf{Q}}$ is the phase associated with $\mathbf{Q}$. The common length q_* of the vectors $\mathbf{Q}$ is approximately equal to the position q_0 of the minimum of the second order vertex function.

4 The vertex functions in the limit of small polydispersity

4.1 Composition fluctuations in the chains

The expressions for the vertex functions can be obtained by straightforward substitution of equation (2) for the block length distribution into the equations derived in [12]. However, the resulting expressions are rather complicated, and in order to gain some physical insight we will study them first for the special cases $k = \infty$ (monodisperse multiblock copolymers), and $k = 1$ (correlated random copolymers). Generally, the second order vertex $\gamma_2(q)$ defined by

$$\Gamma_2(\mathbf{q}_1, \mathbf{q}_2) = V\delta_{\mathrm{K}}(\mathbf{q}_1 + \mathbf{q}_2)\gamma_2(q_1) \qquad (9)$$

has a contribution $\approx q^2$ due to the random walk nature of the chain [23] (δ_{K} is the Kronecker delta). This contribution becomes important for large values of q, corresponding to small length scales. At small length scales the system does not "know" that the A- and B-monomers are connected, and so the q^2-contribution has to be independent of the average block length and the polydispersity. Another important contribution to $\gamma_2(q)$ is long-ranged (small q-values), and is a consequence of the connectivity between the A- and B-blocks. Its form can be derived qualitatively as follows. Consider concentration fluctuations with a given amplitude A, and a large period D. The creation of such fluctuations by stretching individual blocks would cost too much entropy. Therefore, the system uses *effective blocks* [24,25]; that is, long pieces of chain containing a (large) number of A- and B-blocks. The composition of these pieces may differ from the overall composition, even for monodisperse multiblock copolymers, and by rearranging them spatially it is possible to create the desired concentration fluctuation. For monodisperse multiblock copolymers, the composition fluctuation Δf among effective blocks of length N scales like

$$\Delta f \propto \frac{\bar{n}}{N} \qquad \bar{n} \equiv \bar{n}_A + \bar{n}_B. \qquad (10)$$

In principle, the system prefers to use long effective blocks, since this gives rise to smaller entropy penalties. However, in order to create a profile with given amplitude A, the composition fluctuation Δf should at least equal A, leading to an upper bound N_* for the length N of the effective blocks:

$$N \leq N_* \approx \frac{\bar{n}}{A}. \qquad (11)$$

The free energy penalty for stretching an effective block of length N_* over a distance D is $\Delta F = D^2/N_*$ (random

walk statistics). Therefore, the free energy penalty *per unit volume* to create a profile with amplitude A and period D is

$$\Delta F \approx \frac{D^2}{N_*^2} \approx \frac{A^2}{\bar{n}^2 q^2} \, . \tag{12}$$

From the quadratic dependence on A one concludes that this leads to a contribution $1/\bar{n}^2 q^2$ to the second order vertex. Finally, there is a q-independent contribution to γ_2. Combining all terms, we obtain

$$\gamma_2(q) = c + q^2 + \frac{1}{\bar{n}^2 q^2} \tag{13}$$

which is in accordance with rigorous calculations [1]. For the correlated random copolymer (characterized by $k = 1$), the situation is different. In order to find the long-range contribution to the free energy, the same reasoning applies as for the monodisperse case: in order to create large-scale fluctuations with given amplitude A, the system makes use of effective blocks. However, due to the polydisperse block length distribution, the composition variation Δf among effective blocks of length N has a different dependence on N as compared with equation (10)

$$\Delta f \propto \sqrt{\frac{\bar{n}}{N}} \, . \tag{14}$$

Following the same line of reasoning as before, one arrives at:

$$\Delta F \propto \frac{A^4}{\bar{n}^2 q^2} \, . \tag{15}$$

Since this is quartic in A, it gives rise to a contribution $1/\bar{n}^2 q^2$ to the *fourth* order vertex. Rigorous calculations show not only that it indeed exists [6] (it is part of the non-local term Eq. (7)), but also that it is the dominant contribution to the fourth order vertex. It follows that the second order vertex is simply given by

$$\gamma_2(q) = c + q^2 \tag{16}$$

which is consistent with rigorous calculations as well [6]. Summarizing we can say that these qualitative arguments suggest that the $1/\bar{n}^2 q^2$ contribution to the *second* order vertex of monodisperse multiblock copolymers has the same physical origin as the $1/\bar{n}^2 q^2$ contribution to the *fourth* order vertex of correlated random copolymers. The question arises where this contribution is present in case the polydispersity lies in between these two extremes. If the polydispersity is small but non-zero, corresponding to $1 \ll k < \infty$, then *short* pieces of chain are similar to short pieces of monodisperse chains, whereas *long* pieces of chain are essentially polydisperse. Therefore, it is to be expected that on large length scales (small q) the vertex functions resemble those of the correlated random copolymer, whereas on small length scales (large q), they resemble those of the monodisperse multiblock copolymer. It follows that there should exist a critical value q_c

for q at which the $1/\bar{n}^2 q^2$ contribution "jumps" from the fourth order vertex to the second order vertex on increasing q. An estimate for q_c can be obtained by studying the chain composition statistics. For symmetric chains (*i.e.* $f = 1/2$) one can show that the distribution of the number N_A of segments of type A present in a piece of chain containing in total N segments satisfies the relation (see Appendix A)

$$\frac{\langle N_A^2 \rangle - \langle N_A \rangle^2}{\langle N_A \rangle^2} = \frac{\bar{n}}{2kN} + \frac{(k^2 - 4)}{24k^2} \frac{\bar{n}^2}{N^2} + \dots \tag{17}$$

where the dots represent terms which vanish exponentially with increasing value of N. Since k is assumed to be large (small polydispersity), equation (17) reduces to equation (10) if $N \ll k\bar{n}$, while it reduces to equation (14) with renormalized block length $n_* = \bar{n}/k$ if $N \gg k\bar{n}$. In words: pieces of chain containing less than k blocks are essentially monodisperse, while pieces of chain containing more than k blocks are essentially polydisperse. Let R_c be the radius of gyration of a coil containing k blocks. Then the aforementioned critical value q_c is expected to be given by

$$q_c = 1/R_c \approx 1/\sqrt{\bar{n}k}. \tag{18}$$

In terms of the rescaled wave vector $y \equiv \bar{n}q^2$, the critical value is given by $y_c = k^{-1}$. In the next section it is shown that at $y = y_c$ the $1/\bar{n}^2 q^2$ contribution jumps from the fourth order vertex to the second order vertex, in accordance with our qualitative picture.

4.2 The second order vertex

In this section we study the second order vertex function γ_2 for slightly polydisperse multiblock copolymers ($k \gg 1$) in order to test the intuitive idea developed in the previous section. For polydisperse AB-multiblock copolymers the expression for γ_2 is given by [12]

$$\gamma_2(q) = \frac{1}{2\bar{n}} \left[\frac{f(1-f)}{\bar{n}x} - \frac{(1 - \hat{p}_A(x))(1 - \hat{p}_B(x))}{(1 - \hat{p}_A(x)\hat{p}_B(x))\bar{n}^2 x^2} \right]^{-1}$$

$$x = \frac{1}{6} a^2 q^2 = q^2 \tag{19}$$

where $\hat{p}_\alpha(x)$ is the Laplace transform of the block length distribution $p_\alpha(n)$:

$$\hat{p}_\alpha(x) = \int_0^\infty \mathrm{d}n \mathrm{e}^{-nx} p_\alpha(n). \tag{20}$$

For convenience, we define the rescaled wave vector $\tilde{y} \equiv ky = k\bar{n}q^2$. Note that in terms of $\tilde{y}$ the critical wave vector value is given by $\tilde{y}_c = 1$. If we take for $p_\alpha(n)$ the Schultz-Zimm distribution, then for $\tilde{y} \propto 1$ and small polydispersity (large k), the second order vertex equation (19) becomes

$$n\gamma_2(q) \cong \frac{8k}{(1 + \tilde{y}/12)} \, . \tag{21}$$

For $\tilde{y} \gg 1$ equation (21) reduces to $\gamma_2 \approx 1/\bar{n}^2 q^2$, while for $\tilde{y} \ll 1$ the $1/\bar{n}^2 q^2$ contribution disappears, as anticipated.

4.3 The non-local term

Next consider the non-local term Γ_4^{nl}, that, in Fourier representation, can be written as

$$\Gamma_4^{\mathrm{nl}}(\mathbf{q}_1, \mathbf{q}_2, \mathbf{q}_3, \mathbf{q}_4) =$$
$$V\delta_{\mathrm{K}}(\mathbf{q}_1 + \mathbf{q}_2)\delta_{\mathrm{K}}(\mathbf{q}_3 + \mathbf{q}_4)\gamma_4^{\mathrm{nl}}(q_1, q_3) + ... \quad (22)$$

where the dots represent the two remaining terms obtained by permuting $\mathbf{q}_1, ..., \mathbf{q}_4$. The general expression for $\gamma_4^{\mathrm{nl}}(q_1, q_2)$ is rather complicated [12]. However, in the first harmonic approximation one needs it only for $q_1 = q_2$, and for $\tilde{y} \propto 1$, and $k \gg 1$ it simplifies to

$$\bar{n}\gamma_4^{\mathrm{nl}}(q, q) = \frac{128k^3}{\tilde{y}(1 + \tilde{y}/12)^4} \,. \quad (23)$$

Again, there is a change in behavior at $\tilde{y} = 1$. For $\tilde{y} \ll 1$ equation (23) simplifies to

$$\gamma_4^{\mathrm{nl}}(q, q) = \frac{128k^2}{\bar{n}^2 q^2} \quad (24)$$

which coincides, regarding its dependence on q, k and $\bar{n}$, with the expression for the non-local term for a correlated random copolymer with average block length $n_* = \bar{n}/k$. For $\tilde{y} \gg 1$ the non-local term vanishes quickly as $\gamma_4^{\mathrm{nl}} \propto 1/\tilde{y}^5$.

Equation (23) brings forward another interesting feature of the non-local term, concerning its way of convergence in the limit $k \to \infty$. It is well known that the non-local term is absent for monodisperse copolymers, *i.e.*

$$\lim_{k \to \infty} \gamma_4^{\mathrm{nl}}(k, q_1, q_2) = 0. \quad (25)$$

However, it follows from equation (23) that this convergence is *non-uniform*: expressed in terms of the rescaled wave vector $\tilde{y}$ the non-local term *diverges* for $k \to \infty$. The reason for this can be understood in the following way. Let system 1 be characterized by polydispersity k_1^{-1}, and let system 2 be characterized by polydispersity $k_2^{-1} < k_1^{-1}$. Pick from both systems a chain, and consider from both chains a piece with length $N \gg k_2\bar{n}$. Both pieces are polydisperse in the sense defined earlier (*i.e.* with respect to the dependence of Δf on N), and so in both systems the $1/q^2$-term contributes to the *fourth* order vertex on length scales $R \propto \sqrt{N} \gg \sqrt{k_2\bar{n}}$. However, since the chains in system 2 have smaller composition fluctuations than those in system 1, it is more difficult to create concentration fluctuations in system 2 than it is in system 1. Therefore, for $q \ll 1/\sqrt{k_2\bar{n}} \Leftrightarrow \tilde{y} \ll 1$ the non-local term for system 2 must be *larger* than the non-local term for the more polydisperse system 1, despite equation (25).

5 The influence of polydispersity on the phase behavior

5.1 Phase diagrams

In this section we present and discuss the phase diagrams of the polydisperse multiblock copolymers defined in Section 3. The phase diagrams were calculated in the limit
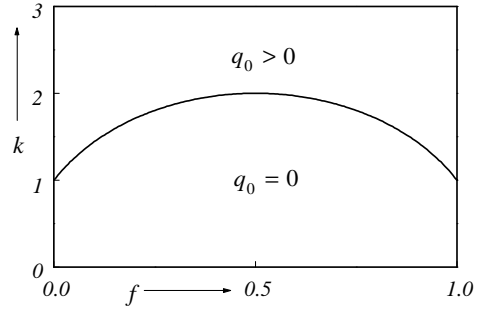

Fig. 2. The line of Lifshitz points. The parameter q_0 is the position of the minimum of the second order vertex. Horizontal axis: *A*-monomer fraction f. Vertical axis: inverse polydispersity k.

$N_{\mathrm{b}} \to \infty$ (N_{b} is the number of blocks per chain). As was shown in [26], the phase diagram for monodisperse multiblock copolymers converges rapidly if the number of blocks increases: once the number of blocks per chain is 10 or larger, the phase diagram is indistinguishable from the limiting one. It is reasonable to assume that the same is true for the polydisperse multiblock copolymers considered in this paper. Due to the polydispersity, the system can in principle macrophase separate into coexisting phases, each of which may be microphase separated. For correlated random copolymers these 2-phase regions were calculated in [17,18], and in [21] the conditions for phase coexistence were derived rigorously for general multiblock copolymers. However, the arising of such a macrophase separated state requires the diffusion of chains as a whole, which is slowed down exponentially if the number of blocks per chain is large [27]. Therefore, in experimental situations the system will remain in a 1-phase state, even if this state is metastable. For this reason the phase diagrams in this paper were constructed under the assumption that the melt remains in a single phase. The aim of this section is to study the influence of polydispersity in the block lengths on the stability of the various structures, and on the periodicity. An important feature is the position q_0 of the minimum of the second order vertex function. For small values of the polydispersity the contribution $1/\bar{n}^2q^2$ is present for small enough q-values to ensure that $q_0 > 0$. For large values of the polydispersity, however, this contribution vanishes too soon for decreasing value of q, leading to $q_0 = 0$. The Lifshitz points (a Lifshitz point is a set of parameter values for which q_0 changes from zero to a non-zero value) in the (f, k)-plane (f is composition, k is the inverse polydispersity) can be found by solving the equation

$$\frac{\mathrm{d}\gamma_2(y)}{\mathrm{d}y} = 0 \quad y \equiv \frac{1}{6}\bar{n}a^2q^2 = \bar{n}q^2. \quad (26)$$

Using equation (19), straightforward calculation shows that the Lifshitz points form a line given by the equation

$$1 + 12f - 12f^2 - k^2 = 0. \quad (27)$$

The location of this line in the (f, k)-plane is shown in Figure 2. It is important to note that even if $q_0 = 0$, the system will undergo a transition to a *micro*phase
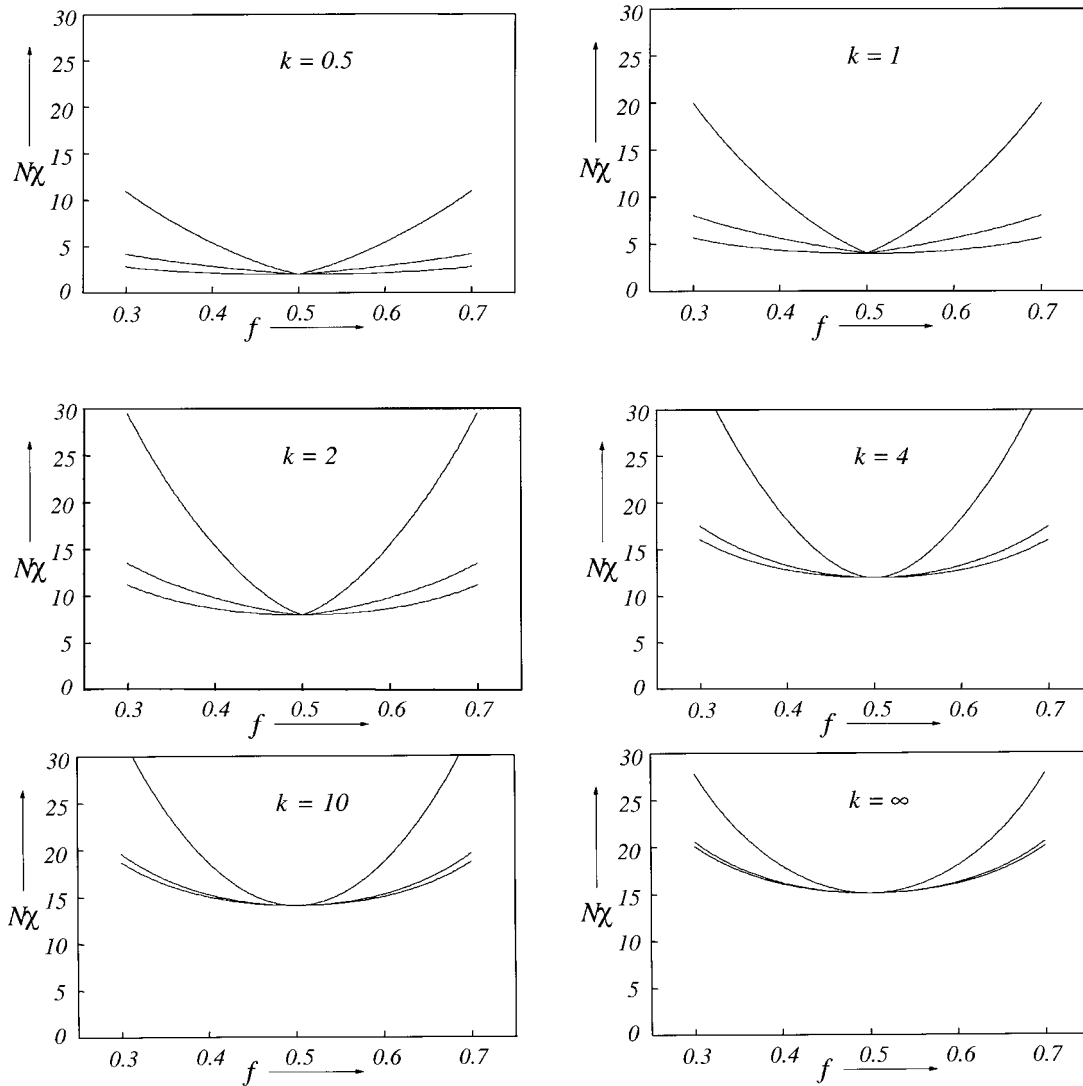
Fig. 3. Mean-field phase diagrams for various values of the inverse polydispersity k. The lower line separates the disordered phase from the BCC phase, the middle line separates the BCC phase from the hexagonal phase, and the upper line separates the hexagonal phase from the lamellar phase. Horizontal: A-monomer fraction f. Vertical axis: product of the Flory-Huggins χ-parameter with the number average total block length $n = n_A + n_B$.

separated state [6] due to the presence of the $1/\bar{n}^2 q^2$-contribution to the fourth order term (non-local contribution). For the situation where the length distribution of the A-blocks is the same as that of the B-blocks, Figure 3 shows weak segregation regime mean-field phase diagrams for various values of the polydispersity $U = k^{-1}$. Figure 4 shows what happens when the length distribution of the A-blocks is monodisperse, while that of the B-blocks is highly polydisperse. These phase diagrams were calculated in the first harmonic approximation by numerically minimizing the Landau free energy with respect to the amplitude and the period of the microstructure. Along the vertical axis we have the product of the χ-parameter with the average total block length $\bar{n} = \bar{n}_A + \bar{n}_B$ (number average). There are several trends visible when the polydispersity is increased.

For instance, the phase transition line shifts down, which seems to indicate that polydispersity destabilizes the homogeneous state. However, this conclusion is not really meaningful, because the vertical axes of the graphs are arbitrary: instead of the number average $\bar{n}$, we could have chosen any other measure for the block length as a prefactor, for instance the harmonic average of the block lengths, the weight average, etc. The direction of the shift of the phase transition line on changing the polydispersity depends on the type of average taken. A real existing trend, however, is the drastic increase in the size of the region of stability of the bcc-phase with respect to that of the hexagonal phase. This increase is related to the fact that for monodisperse copolymers the phase boundaries are smooth at the critical point, while for polydisperse copolymers the phase boundaries have a kink.

5.2 The influence of polydispersity on the period

Consider a symmetric polydisperse multiblock copolymer. Changing the polydispersity while keeping the average block length fixed, the period of the microstructure changes considerably. It is known that for monodisperse multiblock copolymers the period is of the same order of magnitude as the radius of gyration of the blocks, and that it increases slightly on increasing the segregation. For correlated random copolymers, on the other hand, the period is infinite at the spinodal, and decreases sharply with increasing segregation [6]. In the weak segregation regime the period is much larger than the average radius of gyration of the blocks. This is because the microstructure is constructed from "effective blocks", [24,25] each consisting of a large number of A- and B-blocks. As the segregation strength increases, the system wants to increase the separation between the A- and B-monomers. Since short pieces of chain have larger composition fluctuations than long pieces of chain, the system has to use shorter effective blocks in order to increase the separation, which leads to a shorter period. Figure 5 shows, for $f = 1/2$, how the period changes with the interaction strength for various values of the polydispersity.

6 Summary

We studied theoretically the influence of polydispersity in block length on the phase behavior of binary multiblock copolymer melts. For the reasonable case of Schultz-Zimm block molecular weight distributions, we presented the expressions for the vertex functions, and provided simple physical arguments to explain these expressions qualitatively. We predict a dramatic increase of the region of stability of the bcc phase with increasing polydispersity, which is related to the fact that for non-zero polydispersity the phase boundaries have a kink at the critical point. In order to confirm our mean-field predictions experimentally, it should be kept in mind that since polydispersity enhances the influence of fluctuations, one has to study multiblock copolymers with sufficiently long average block length.

7 Outlook

The analysis presented here can be extended in several ways. The phase diagrams in Figure 3 could be improved by taking into account the effect of higher harmonics [2]. This might lead to interesting results because the higher harmonics stabilize complex phases like the gyroid phase, while in the first harmonic approximation one can only predict regions of stability of the classical structures lamellar, hexagonal and bcc. The polydispersity might have a large influence on the stability of these complex structures (according to Fig. 3 it has a large influence on the stability of the bcc-phase). Another extension is to calculate the weak segregation phase diagrams for multiblock copolymers consisting of more than two monomer types. It was shown in [12] that close to the spinodal the coarse grained state of such multi-component systems can still be
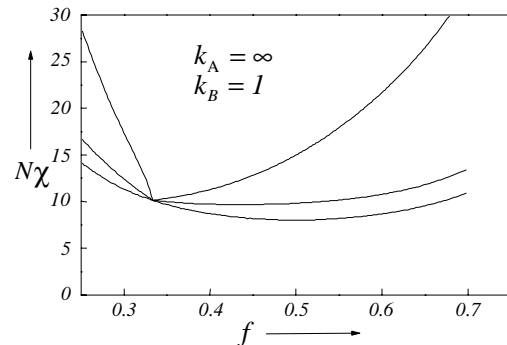

Fig. 4. Mean-field phase diagram for the situation where the A-blocks are highly polydisperse, while the B-blocks are monodisperse. Horizontal: A-monomer fraction f. Vertical axis: product of the Flory-Huggins χ-parameter with the number average total block length $n = n_A + n_B$.
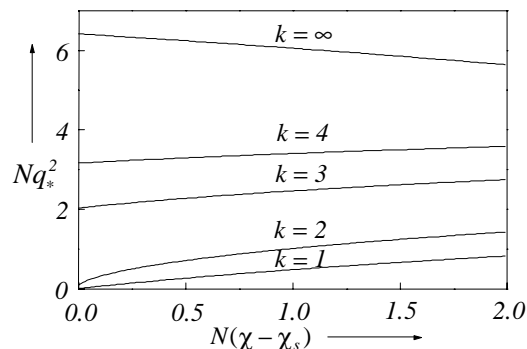

Fig. 5. The dependence of the periodicity $D = 2\pi/q_*$ on the polydispersity and on the interaction strength. Horizontal axis: the rescaled distance to the spinodal ($n = n_A + n_B$ is the number average block length, and χ_s is the spinodal value of χ). Vertical axis: rescaled q-vector.

described by means of just one order parameter field, and so the weak segregation phase diagram can be calculated along the same lines as for the 2-component case.

Appendix A

In this appendix an expression is derived for the composition fluctuation Δf in pieces of chain as a function of their length N, where Δf is defined by

$$\Delta f = \frac{\langle N_A^2 \rangle - \langle N_A \rangle^2}{\langle N_A \rangle^2} . \qquad (A.1)$$

N_A is the number of A-segments among the total number of N segments, and the brackets denote an average over one infinite chain. There are several possibilities for the state ω of this piece of chain: it could consist entirely of A-monomers, or it starts with an A-block, ends with a B-block, with any number of blocks in between, etc. Let $P(N, \omega)$ denote the probability to find the state ω, and

$N_A(\omega)$ the number of A-segments corresponding to the state ω. Define the generating functional W by

$$W(N, z) = \sum_\omega e^{zN_A(\omega)} P(N, \omega) \qquad \text{(A.2)}$$

then the averages $\langle N_A^i \rangle$ can be obtained by (repeated) differentiation of W, after which the averages $\langle N_B^i \rangle$ follow from $N_B = N - N_A$. The summation over ω can be split into 6 subsummations. As an example we consider the subsummation over all ω which start and end with an A-block, with $(t - 2) \geq 0$ A-blocks and $(t - 1)$ B-blocks in between. The corresponding subset of Ω is denoted by Ω_{AA}. Let n_i be the number of segments in the ith A-block, and m_i the number of segments in the ith B-block, then the probability $P(N, \omega)$ is given by

$$e^{zN_A(\omega)} P(N, \omega) = \frac{1}{n_A + n_B}$$
$$\times \int_{n_1}^\infty p_A(x)\mathrm{d}x \, p_B(m_1) p_A(n_2) p_B(m_2) ... p_A(n_{t-1}) p_B(n_{t-1})$$
$$\times \int_{n_t}^\infty p_A(y)\mathrm{d}y \exp[z(n_1 + ... + n_t)]$$
$$\times \delta_\mathrm{D}(n_1 + m_1 + n_2 + m_2 + ... + m_{t-1} + n_t - N). \qquad \text{(A.3)}$$

Due to the Dirac delta function, the integrals over n_i and m_i (which arise in the summation over ω in Eq. (A.2)) are coupled. They can be decoupled by performing a Laplace transformation with respect to the variable N, leading to

$$\sum_{\omega \in \Omega_{AA}} e^{zN_A(\omega)} \hat{P}(s, \omega) = \frac{1}{n_A + n_B}$$
$$\times \sum_{t=2}^\infty \hat{Q}_A^2(s - z) \hat{p}_A^{t-2}(s - z) \hat{p}_B^{t-1}(s)$$
$$= \frac{1}{n_A + n_B} \frac{\hat{Q}_A^2(s - z) \hat{p}_B(s)}{1 - p_A(s - z) p_B(s)}$$

$$Q_\alpha(n) = \int_n^\infty p_\alpha(x)\mathrm{d}x \qquad \hat{Q}_\alpha(s) = \frac{1 - \hat{p}_\alpha(s)}{s} . \qquad \text{(A.4)}$$

The summations over Ω_{AB}, Ω_{BA} and Ω_{BB} can be handled in the same way. There remain the subsets Ω_α, each consisting of only one state ω in which all segments are of type α. The probability of this state is

$$P_\alpha(N, \omega) = \frac{1}{(n_A + n_B)} \int_N^\infty \mathrm{d}n(n - N) p_\alpha(n). \qquad \text{(A.5)}$$

Therefore,

$$\sum_{\omega \in \Omega_A} e^{zN_A(\omega)} \hat{P}(s, \omega) = \frac{\hat{p}_A(s - z) - 1 + (s - z)n_A}{(s - z)^2} . \qquad \text{(A.6)}$$

Adding all contributions, and filling in the Schultz-Zimm distribution

$$p_\alpha(n) = \frac{k^k e^{-kn/\bar{n}_\alpha} n^{k-1}}{\Gamma(k) \bar{n}_\alpha^k} \Leftrightarrow p_\alpha(s) = \frac{1}{\left(1 + \frac{\bar{n}_\alpha s}{k}\right)^k} \qquad \text{(A.7)}$$

one obtains finally, after differentiation with respect to z followed by an inverse Laplace transformation

$$\frac{\langle N_A^2 \rangle - \langle N_A \rangle^2}{\langle N_A \rangle^2} = \frac{2(1 - f)^2 \bar{n}}{kN}$$
$$+ \frac{(1 - f)^2(-1 - 12f + 12f^2 + k^2)\bar{n}^2}{6k^2 N^2} + ... \qquad \text{(A.8)}$$

where the dots denote terms which vanish exponentially with N. Note that a Lifshitz point occurs when the second term on the right hand side vanishes (see Eq. (27) and Fig. 2).

References

1. L. Leibler, Macromolecules **13**, 1602 (1980).
2. M. Olvera de la Cruz, A.M. Mayes, B.W. Swift, Macromolecules **25**, 944 (1992).
3. G.H. Fredrickson, E. Helfand, J. Chem. Phys. **87**, 697 (1987).
4. M.W. Matsen, F.S. Bates, Macromolecules **29**, 1091 (1996).
5. H. Benoit, G. Hadziioannou, Macromolecules **21**, 1449 (1988).
6. E.I. Shakhnovich, A.M. Gutin, J. Phys. France **50**, 1843 (1989).
7. G. Burger, W. Ruland, A.N. Semenov, Macromolecules **23**, 3339 (1990).
8. S.V. Panyukov, S.I. Kuchanov, JETP **72**, 368 (1991).
9. S.V. Panyukov, S.I. Kuchanov, JETP Lett. **54**, 501 (1991).
10. S.V. Panyukov, S.I. Kuchanov, J. Phys. II France **2**, 1973 (1992).
11. I.Ya. Erukhimovich, A.V. Dobrynin, Macromol. Symp. **81**, 253 (1994).
12. J.J.M. Slot, H.J. Angerman, G. ten Brinke, (submitted to J. Chem. Phys.)
13. G.H. Fredrickson, S.T. Milner, L. Leibler, Macromolecules **25**, 6341 (1992).
14. C.D. Sfatos, A.M. Gutin, E.I. Shakhnovich, Phys. Rev. E **51**, 4727 (1995).
15. A.M. Gutin, C.D. Sfatos, E.I. Shakhnovich, J. Phys. A **27**, 7957 (1994).
16. S.V. Panyukov, I.I. Potemkin, JETP Lett. **64**, 197 (1996).
17. S.V. Panyukov, I.I. Potemkin, (preprint).
18. S.V. Panyukov, I.I. Potemkin, JETP **85**, 183 (1997).
19. H.J. Angerman, G. ten Brinke, I.Ya. Erukhimovich, Macromolecules **29**, 3255 (1996).
20. H.J. Angerman, G. ten Brinke, I.Ya. Erukhimovich, Macromolecules **6**, 1958 (1998).
21. H.J. Angerman, G. ten Brinke, I.Ya. Erukhimovich (to be published).
22. L.D. Landau, I.M. Lifshitz, *Statistical Physics* (Addison-Wesley, Reading, MA, 1969).
23. P.G. De Gennes, *Scaling Concepts in Polymer Physics* (Cornell University Press, 1979).
24. H.J. Angerman, Ph.D. thesis, University of Groningen, 1998.
25. A.N. Semenov, J. Phys. II France **7**, 1489 (1997).
26. A.V. Dobrynin, I.Ya. Erukhimovich, Macromolecules **26**, 276 (1993).
27. J.P. Bouchaud, M.E. Cates, J. Phys. II France **3**, 1171 (1993).